

Photorefractive cyclometalated complexes

R. TERMINE¹, M. TALARICO², I. AIELLO², D. DATTILO², D. PUCCI*², M. GHEDINI²,
and A. GOLEMME²

¹Centro di Eccellenza CEMIF.CAL, Sezione INSTM della Calabria
Laboratorio Regionale Licryl CNR-INFM, Italy

²Dipartimento di Chimica, Università della Calabria, 87030 Rende, Italy

Some of the most recent results on the photoconducting and photorefractive properties of cyclometalated complexes are reviewed. Pure compounds show good photoconducting properties, which can be increased by orders of magnitude by doping with fullerenes. In addition, photorefractivity has been observed both in pure materials in their glassy state and in mixtures with inert polymers. In such mixtures, at high concentrations of complexes, dispersions of small (less than 200 nm) crystals of the complex within a polymeric matrix can be obtained. This morphology has been clearly linked to an increase in photorefractive performance, measured through diffraction efficiency, by orders of magnitude. Moreover, complexes with proper ligands exhibit chiral smectic mesophases with ferroelectric properties which also show photorefractive properties.

Keywords: photoconductivity, photorefractivity, cyclometalated complexes.

1. Introduction

One of the most widely explored research lines in recent years has been conducted with the background target of substituting electronics with photonics, since, in principle, photons can carry much more information and more rapidly than electrons. Within this frame, materials with physical properties that can be modulated by light are very interesting, among these are photoconducting media [1], which exhibit a light dependent electric conductivity. They can be used as materials for detectors and other simpler devices and, what is more important, they can show more complex behaviour such as in photorefractivity or photovoltaics.

Ideally, a photoconductor should be an insulator in the dark and became a conductor when illuminated via the photogeneration of charge carriers (electrons or holes, less often both of them). In crystalline materials, the ordered structure is reflected in the formation of different energy bands and photogenerated carriers can easily contribute to conductivity. In organic materials, photogenerated charges can instead diffuse only by hopping between localized states. In addition, the quantum efficiency of the processes which follow light absorption and lead to charge separation is limited in organics by their low dielectric constants. These factors determine the reduced values of photoconductivity in organic semiconductors, when they are compared to inorganic crystals. Nonetheless, the advantages offered by several features of organic materials, including low cost, mechanical flexibility and processability, have

propelled research aimed at understanding and improving their photoconductivity.

In this paper, we will illustrate the properties of a new class of organic materials showing photoconductive and photorefractive (PR) properties. PR media, where non-local refractive index patterns (holograms) can be recorded by light, can be useful both for permanent and dynamic holographic applications ranging from optical memories to image treatment [2,3]. In this work, the PR properties of cyclometalated complexes with a square-planar geometry, some of which are shown in Fig. 1, will be described. Depending on the nature of the ligands, different aggregation forms are possible for such compounds, as stable or metastable states, including crystalline, glassy and liquid crystalline phases, with a variety of different features, most of which are interesting for photorefractivity.

2. Materials, sample preparation, and experimental techniques

Since light does not propagate through scattering media, experimental investigations of light induced properties require homogeneous samples. The complexes shown in Fig. 1 are microcrystalline at room temperature, and strongly scatter visible light. With the complexes shown in Figs. 1(b) and 1(c) it is possible to obtain amorphous samples by melting the material and its rapid cooling down to a room temperature, while the complex shown in Fig. 1(a) does not show any stable glassy state and in order to obtain amorphous samples it is necessary to dissolve it within inert polymers. For this purpose we used poly(vinyltoluene-

* e-mail: d.pucci@unical.it

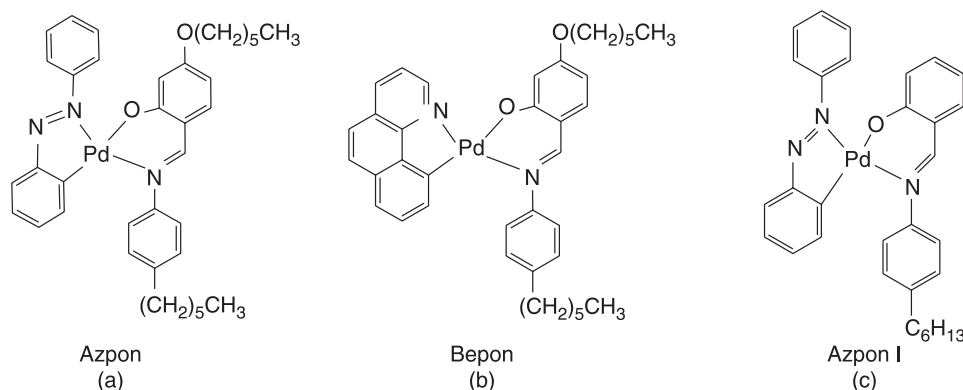


Fig. 1. Chemical structure of the cyclometalated complexes used. There is a square planar geometry around the central metal atom.

co- α -methylstyrene) (PVTMS) or poly(isobutyl methacrylate) (PIBMA) (Aldrich), purified by recrystallization before the use. In order to minimize the quantity of inert material, we kept the concentration of complex just below the limit for which macroscopic phase separation was observed under a microscope. Amorphous samples are obtained by firstly, dissolving the proper quantities of polymer and complex in chloroform, allowing for the complete solvent evaporation, sandwiching the hot melt between two ITO coated glasses (controlling the thickness with glass spacers) and secondly, cooling down rapidly. Samples were finally observed by using a polarized optical microscope to check for phase homogeneity.

Photoconduction measurements were conducted by measuring the difference in electric conductivity upon illuminating samples with light at 633 nm. In order to compare the results obtained at different light intensities I and with samples having different absorption coefficients α , the photoconductivity σ is normalized with respect to I and α .

To characterize photorefractive properties, degenerate four-wave mixing (FWM) and two-beam coupling (2BC) experiments were performed. In both cases, an interference pattern was created by overlapping on the samples two He-Ne laser beams, each one with the power density $I \sim 0.5 \text{ W cm}^{-2}$. As usual, with organic materials, a DC external field was applied and in order to have a component of the applied field along the grating wavevector, the sample normal was tilted 60° away from the bisector of the beams. The grating period $\Lambda \sim 3 \mu\text{m}$ was selected by properly choosing the angle between the beams. FWM experiments were performed by using a weak p-polarized 'reading' beam which was counterpropagating with respect to one of the two s-polarized "writing" beams. The reading beam originated from the same He-Ne laser as the writing beams and its power density was $I \sim 5 \times 10^{-4} \text{ W cm}^{-2}$. The diffraction efficiency η , which is measured in FWM, is defined as the ratio between the diffracted and the total reading beam intensity.

Two-beam coupling (2BC) is the experiment that confirms the photorefractive nature of a grating, the phase shift between interference fringes and grating induces an asymmetric energy exchange between the beams, measured by the gain coefficient which can be experimentally obtained as

$$\Gamma = d_1 \ln \frac{I_1(I_2 \neq 0)}{I_1(I_1 = 0)} - d_2 \ln \frac{I_2(I_1 \neq 0)}{I_2(I_1 = 0)}, \quad (1)$$

where d_1 and d_2 are the paths of beam 1 and 2 in the sample, respectively, and $I_1(I_2 \neq 0)$ and $I_1(I_2 = 0)$ are the intensities of beam 1 beyond the sample with beam 2 on and off, respectively. Similar definitions apply to $I_2(I_1 \neq 0)$ and $I_2(I_1 = 0)$.

Ellipsometric measurements were performed by exposing the sample to a single light beam incident under the internal angle $\beta = 26^\circ$ with respect to the sample normal and by setting the beam polarization at $+45^\circ$ with respect to the plane defined by the sample normal and the propagation direction of the light. A second polarizer set at -45° was placed after the sample while a compensator, between this last polarizer and the sample was set so that no light intensity could be detected after the second polarizer. If the refractive index of the sample is changed by an applied electric field, then the initially isotropic sample will develop optical anisotropy and will act as a phase retarder. This causes a change in polarization of the light, that is then not completely blocked by the second polarizer. When a biased AC electric field is applied and the modulation of the transmitted light intensity is measured versus the frequency of the electric field, it is possible to infer the physical origin of the light induced refractive index variation. In the case of NLO effects, the light intensity varies with the field even at high frequencies, while reorientations of molecules, or molecular aggregates, are inactive at frequencies above a few tens or hundreds of Hz. With the same set-up, but applying a DC field, it is possible to measure the field dependence of the refractive index Δn seen by the light beam, by using

$$\Delta n = \frac{\lambda \cos \beta}{2\pi d} \arcsin \sqrt{\frac{I}{I_{\max}}}, \quad (2)$$

where d is the thickness of the sample, λ is the wavelength of the light, β is the angle between the sample normal and the light direction, I is the light passing through the setup at the given electric field and I_{\max} is the maximum light intensity passing through the system, measured by changing the phase retardation of the compensator.

3. Photoconductivity and photorefractivity in cyclometalated complexes

3.1. Photoconductivity

Photoconductivity in different samples was measured as described previously. The inset of Fig. 2(a) shows the normalized photoconductivity in the case of BEPON, it is possible to note the strong dependence of photoconduction on the applied electric field. This behaviour is typical for organic photoconductors [4] and it is generally attributed mainly to field-enhanced photogeneration. In fact, because of the low dielectric constant typical for organic material, recombination processes of photogenerated excitons can occur easily, dumping charge generation, while exciton dissociation into “free” carriers is boosted by an applied electric field.

It should be underlined that the $\sigma/\alpha I$ values for the materials analyzed in the present paper are comparable to the values reached for typical amorphous organic photoconductors. One of the most extensively studied photoconducting polymers is polyvinylcarbazole (PVK), often doped with trinitrofluorenone (TNF) as a photosensitizer. In the samples containing also the disperse red 1 dye with the composition PVK:DR1:TNF = 75:24:1, the ratio $\sigma/\alpha I$ reaches the value $4.4 \times 10^{-13} \text{ cm}^2 \Omega^{-1} \text{ W}^{-1}$ at $100 \text{ V}/\mu\text{m}$ [5]. The comparison with other known photoconductors becomes even better if we dope our cyclopalladated complexes with C_{60} , which is well known to promote hole conduction by stabilizing electrons. Samples of both AZPON:PIBMA = 60:40 and BEPON containing $\sim 1\%$ of C_{60} were prepared. At this concentration, the absorption coefficient is only slightly increased by the dopant addition but in both cases photoconductivity increases by orders of magnitude, as shown in Fig. 2. In particular, for an applied field $E \sim 100$

$\text{V}/\mu\text{m}$, $\sigma/\alpha I \sim 1.2 \times 10^{-12} \text{ cm}^2 \Omega^{-1} \text{ W}^{-1}$ for BEPON, increasing by two orders of magnitude, while in the case of AZPON the addition of C_{60} makes the photoconductivity measurable and $\sigma/\alpha I = 1.58 \times 10^{-15} \text{ cm}^2 \Omega^{-1} \text{ W}^{-1}$ for the same value of applied field.

3.2. Photorefractivity

The photorefractive (PR) effect is the spatial modulation of the refractive index by an electric field obtained via a non-uniform illumination [2,3]. PR media are photoconductors, in which light absorption induces the formation of mobile charge carriers that diffuse or drift through macroscopic distances establishing a charge distribution and the related internal electric field, called space-charge field E_{sc} . If the refractive index can be modified by E_{sc} , a refractive index replica (hologram) of the light pattern will be encoded in the material. The phenomena leading to the field dependent refractive index modulation are usually classified as non-linear optical (NLO) or reorientational. The original light pattern and the resulting hologram are shifted in space by the phase factor ϕ , the term non-local, which usually describes the PR holograms, underlines the existence of this spatial shift. There are a number of different physical phenomena that can produce light-induced refractive index modulations but the PR mechanism is the only one known to lead to non-local holograms, with important and technologically relevant consequences. After being extensively studied in inorganic crystals, more recently the photorefractive properties of organic crystalline [6] and amorphous [7] materials became the subject of intense research efforts [8].

In Fig. 3, we show the results of 2BC experiments in AZPON/PIBMA and BEPON samples. It is clear that increasing the applied electric field, the exchange in energy between the two beams increases demonstrating the PR

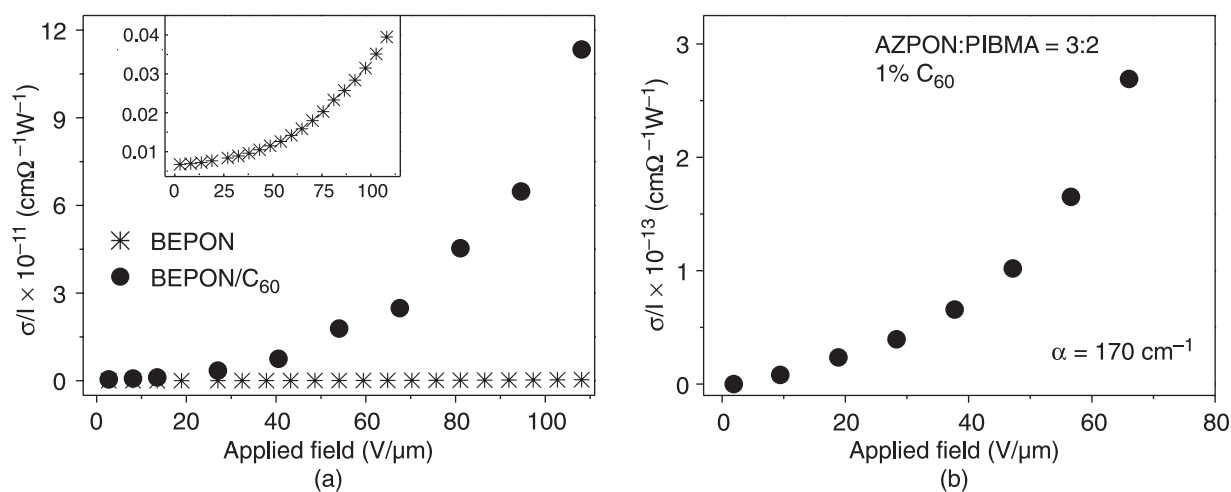


Fig. 2. Normalized photoconductivity versus applied electric field in pure BEPON and BEPON doped with C_{60} (a). The absorption coefficient α of the pure sample is $\alpha = 49 \text{ cm}^{-1}$, while in the doped sample $\alpha = 96 \text{ cm}^{-1}$. The applied field dependence of the normalized photoconductivity of the undoped sample is shown in the inset on a different scale. Normalized photoconductivity versus applied electric field in AZPON:PIBMA = 3:2 doped with C_{60} (b).

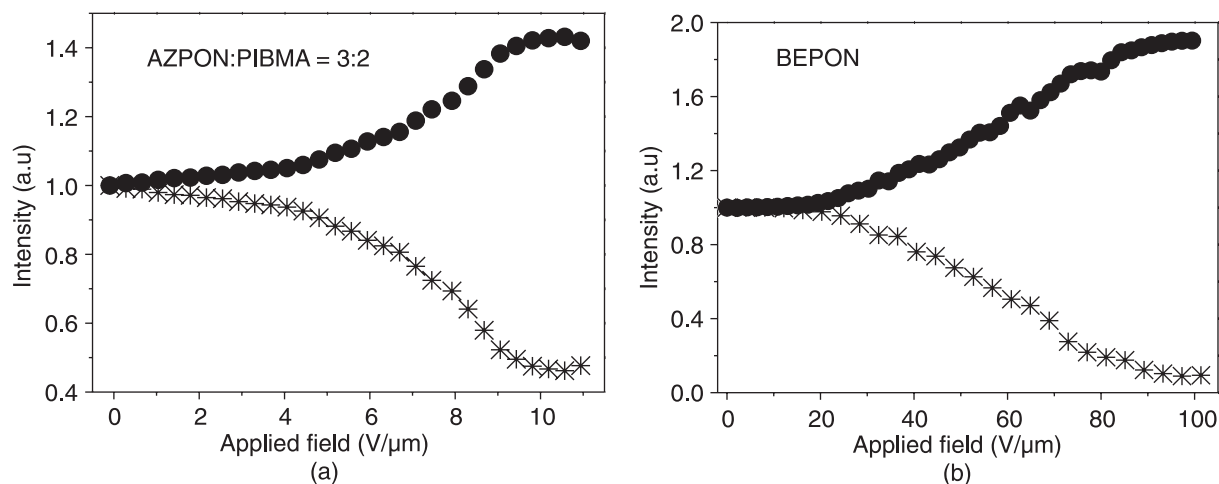


Fig. 3. Two-beam coupling measurements in AZPON/PIBMA (a) and BEPON (b) versus the external electric field.

nature of the grating [9]. For BEPON-Pd, the gain coefficient $\Gamma = 750 \text{ cm}^{-1}$ was obtained, the highest among the measured in organic amorphous materials [10]. The origin of the PR properties in these materials was assessed through different experimental routes, as discussed in the following. The applied field dependence of diffraction efficiency was measured at different temperatures for AZPON/PIBMA and BEPON and, as shown in Fig. 4, there is a strong variation of the efficiency with temperature, indicating the importance of reorientational effects. In order to establish more in detail the nature of such effects, AC ellipsometric measurements were performed and, as shown in Fig. 5, upon increasing the frequency of the field, the intensity of the light modulation at the same frequency of the field drops rapidly, clearly indicating that the refractive index modulation is due to reorientational mechanisms.

In Fig. 6, the results of DC ellipsometric measurements are illustrated. The birefringence of AZPON/PIBMA shows a step-like increases for applied fields $5 < E < 15 \text{ V}/\mu\text{m}$, superimposed to the usual more regular field de-

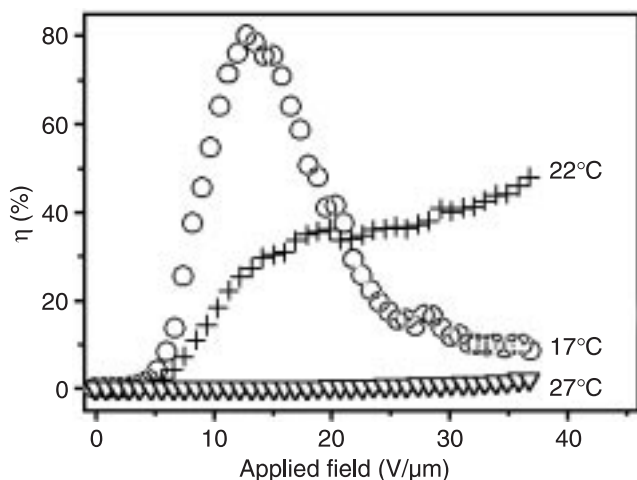


Fig. 4. Applied electric field dependence of the diffraction efficiency η in AZPON:PIBMA = 3:2 at different temperatures.

pendence. Moreover, a similar step-like trend at similar values of the field can also be observed in the energy exchange, Fig. 3(a), and diffraction efficiency, Fig. 4(a). The evidence points towards the existence of some sort of reorientational effects which is completed for $E \sim 20 \text{ V}/\mu\text{m}$ and, since at these fields the dipole reorientational energy is several orders of magnitude lower than thermal energy (even for large molecular dipoles), the existence of crystalline domains of AZPON was supposed [11]. In this case the complete reorientation of crystalline domains would require lower field values because the reorientation energy F is not anymore tied to molecular dipole orientation but to the dielectric anisotropy $\Delta\epsilon$

$$F = 1/2 \epsilon_0 |\Delta\epsilon| E^2 V, \quad (3)$$

where V is the volume of the crystal. Since samples appear homogeneous when observed with an optical microscope,

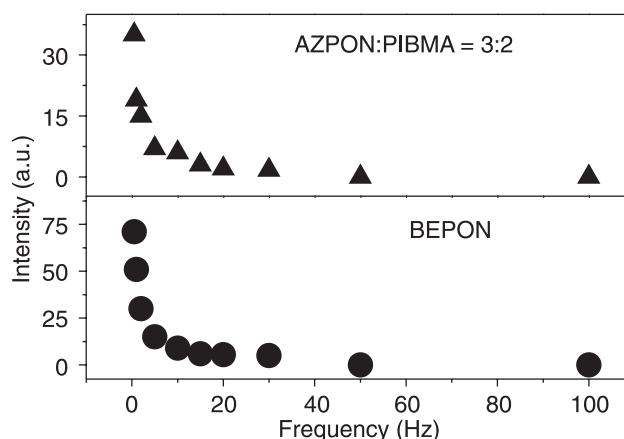


Fig. 5. Refractive index modulation in ellipsometric measurements on AZPON:PIBMA = 3:2 (a) and BEPON (b). Experiments were carried out by applying biased AC electric fields of different frequency and following on a lock-in amplifier the field induced signal modulation at the same frequency of the field, as described in the text.

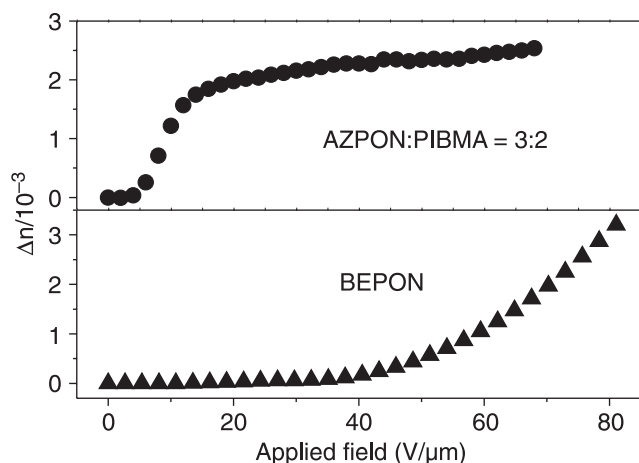


Fig. 6. Induced birefringence versus applied DC electric field in AZPON:PIBMA = 3:2 and BEPON, measured in ellispometric measurements as described in the text.

the size of the crystalline domains should be lower than 200–300 nm. X-rays measurements confirmed the presence of crystalline domains, as shown in Fig. 7, more and more evident as the concentration of AZPON in PIBMA increases. Further evidence of the importance of the dispersed morphology comes from the data obtained from the complex of Fig. 1(c). In this case, a highly photoconducting, very stable glassy phase is obtained in the pure compound but, due to the absence of crystalline domains, its PR performance is rather poor. Usually, phase separation is detrimental in PR organic composites since large enough domains scatter light. These results constitute the first evidence that, if carefully controlled, phase separation can be extremely useful and that the resulting materials with a dispersed morphology can have outstanding PR performance.

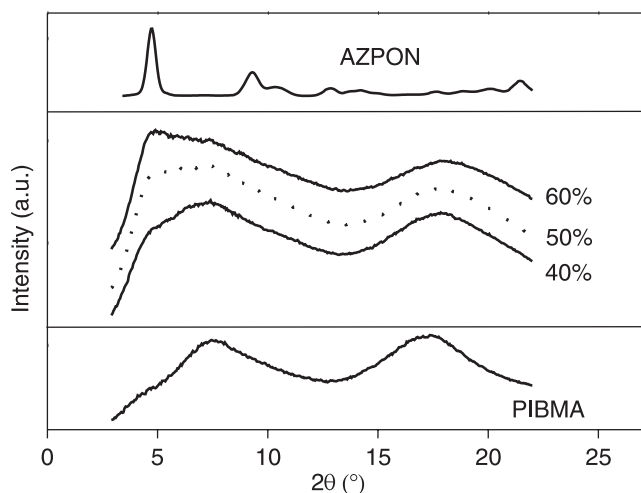


Fig. 7. X-ray diffraction patterns for pure AZPON (upper trace), pure PIBMA (lower trace) and AZPON dissolved in PIBMA at different concentrations. The weight concentrations reported indicate AZPON content.

3.3. Photorefractivity in mesophases

The ligands, and their alkyl or alkoxy terminal chains, of cyclometallated complexes can of course be chosen in order to induce different properties. This can be done, for example, to obtain liquid crystalline phases [12]. The compound shown in Fig. 8(a) exhibits a chiral Nematic and a chiral Smectic C (SmC^*) phase [13], the last one particularly interesting since it is a ferroelectric phase in which spontaneous polarization can be reoriented by a space-charge electric field, as illustrated in Fig. 8(b). Two-beam coupling experiments were performed at 63°C, well within the smectic C^* mesophase [14]. The energy exchange (Fig. 9) between the laser beams confirms the photorefractive nature of the grating recorded in the material. From these data the gain coefficient Γ can be measured and we obtain $\Gamma = 125 \text{ cm}^{-1}$. In addition, a phase shift $\theta = 30 \pm 5^\circ$ between the light pattern and grating was measured by using the moving-grating technique [6]. Since Γ and θ are related by

$$\Gamma = \frac{2\pi}{\lambda} \Delta n_G \sin \theta, \quad (4)$$

Δn_G , the amplitude of refractive index modulation, could be obtained.

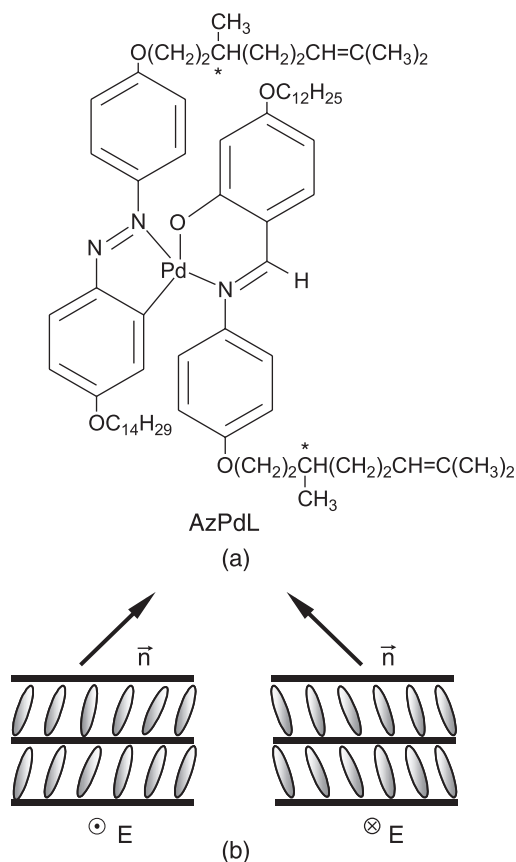


Fig. 8. Chemical structure of the cyclometalated complex AzPdL, which exhibits a chiral smectic C mesophase (a) and schematic representation of the molecular reorientation in SmC^* mesophases under the effect of an electric field (b).

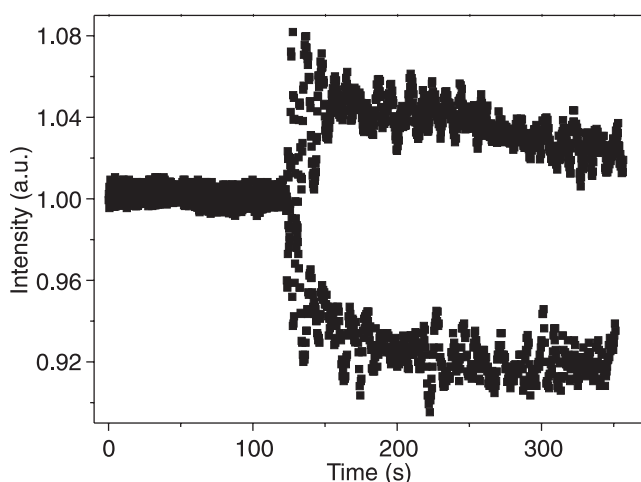


Fig. 9. Time dependence of two-beam coupling in a sample of AzPdL. At the time $t = 120$ s an electric field $E = 5.4$ V/ μm is turned on with the sample illuminated by two coherent overlapping light beams from a He-Ne laser.

Measurements were performed for different light polarizations and they compare well with a model developed to describe director reorientation in ferroelectric smectics due to sinusoidal space-charge fields [15]. The comparison of experimental and calculated data is shown in Fig. 10.

The only fitting parameter in the model used to derive the fitting shown in Fig. 10 is the ratio k between space-charge field inside the material and the applied external field, the value $k = 9 \pm 1 \times 10^{-3}$ was obtained [16]. These photogenerated fields can be derived by using two different approaches. One of them was developed to take into account the specific photogeneration and charge carrier trans-

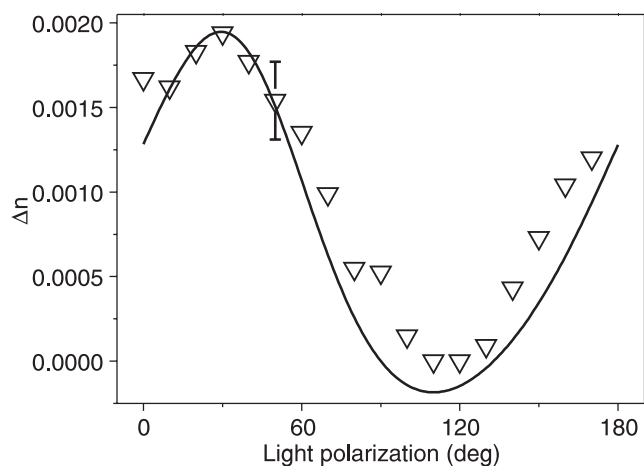


Fig. 10. Refractive index modulation Δn (full line) calculated by using the model described in Ref. 15 and refractive index modulation Δn measured as a function of the polarization of the writing beams at $E = 5.4$ V/ μm (dots), obtained by using Eq. (4) from experimentally determined values of the phase mismatch θ and the gain coefficient Γ . The best fit with the experimental data corresponds to a ratio between space-charge and applied fields $k = 8.5 \times 10^{-3}$.

port properties of organic materials [4,17,18], but it is difficult to use because it considers a series of parameters which are unknown or difficult to measure. For this reason, in most cases the simpler models developed for inorganic crystals [2,3] are used also to describe space-charge fields in amorphous organics. If we use such an approach [16], we get $k \sim 0.85$. The difference is of two orders of magnitude and this fact suggests that the extension to organic materials of concepts, which are well established for inorganics, should be considered with more caution.

4. Conclusions

The photoconduction properties of a new class of materials, cyclometalated complexes have been presented. Measurements were conducted on amorphous samples of the pure compounds as well as in mixtures with inert polymers and in samples doped with C_{60} . The photorefractive behaviour of two model complexes were discussed and, within this frame, the properties induced by a material morphology in which crystalline domains of the complex are dispersed within a photoconducting amorphous matrix were illustrated. This morphology was obtained by controlled phase separation and, if the size of the dispersed domains is below ~ 200 nm, scattering in the visible is avoided while, at the same time, the reorientation of the domains can be observed at much lower fields when compared to the reorientation of molecular dipoles. The photorefractive properties exhibited by molecules belonging at the same chemical class in a ferroelectric Smectic C^* mesophase were also discussed. In this case, by using a simple model it was possible to derive the amplitude of the photoinduced space-charge field.

References

1. N.V. Joshi, *Photoconductivity*, Dekker, New York, 1990.
2. P. Yeh, *Introduction to Photorefractive Nonlinear Optics*, Wiley, New York, 1993.
3. L. Solymar, D.J. Webb, and A. Grunnet-Jepsen, *The Physics and Applications of Photorefractive Materials*, Clarendon, Oxford, 1996.
4. G. Montemezzani, C. Medrano, M. Zgonik, and P. Günter, "The photorefractive effect in inorganic and organic materials", in *Nonlinear Optical Effects and Materials*, pp. 301–373, edited by P. Günter, Springer-Verlag, Berlin, 2000.
5. B. Kippelen, K. Meerholz, and N. Peyghambarian, "An introduction to photorefractive polymers", in *Nonlinear Optics of Organic Molecules and Polymers*, pp. 465–513, edited by H.S. Nalwa and S. Miyata, CRC Press, Boca Raton, 1997.
6. K. Sutter, P. Günter, "Photorefractive gratings in the organic crystal 2-cyclooctylamino-5-nitropyridine doped with 7,7,8,8-tetracyanoquinodimethane", *J. Opt. Soc. Am.* **B7**, 2274–2278 (1990).
7. S. Ducharme, J.C. Scott, R.J. Twieg, and W.E. Moerner, "Observation of the photorefractive effect in a polymer", *Phys. Rev. Lett.* **66**, 1846–1849 (1991).

8. O. Ostroverkhova and W.E. Moerner, "Organic photorefractives: mechanisms, materials and applications", *Chem. Rev.* **104**, 3267–3314 (2004).
9. I. Aiello, D. Dattilo, M. Ghedini, and A. Golemme, "Cyclo-metalated complexes: a new class of highly efficient photorefractive materials", *J. Am. Chem. Soc.* **123**, 5598–5599 (2001).
10. I. Aiello, D. Dattilo, M. Ghedini, A. Bruno, R. Termine, and A. Golemme, "Cyclopalladated complexes as photorefractive materials with high refractive index modulation", *Adv. Mater.* **14**, 1233–1236 (2002).
11. R. Termine, I. Aiello, D. Dattilo, M. Ghedini, and A. Golemme, "Photorefractive performance enhancement in polymer dispersions of nano-size crystalline domains", *Adv. Mater.* **15**, 723–726 (2003).
12. M. Ghedini, D. Pucci, E. Cesarotti, O. Francescangeli, and R. Bartolino, "Transition metals complexed to ordered mesophases XIII. Synthesis and mesomorphic properties of potentially ferroelectric Schiff's base Palladium(II) complexes", *Liq. Cryst.* **15**, 331–344 (1993).
13. D. Pucci, O. Francescangeli, and M. Ghedini, "Heteroligand palladium complexes with one or two chiral centres", *Mol. Cryst. Liq. Cryst.* **372**, 51–68 (2001).
14. M. Talarico, G. Barberio, D. Pucci, M. Ghedini, and A. Golemme, "Undoped photorefractive ferroelectric liquid crystal", *Adv. Mater.* **15**, 1374–1377 (2003).
15. R. Termine and A. Golemme, "Photorefractive index modulation in chiral smectic phases", *J. Phys. Chem.* **B106**, 4105–4111 (2002).
16. M. Talarico, R. Termine, G. Barberio, D. Pucci, M. Ghedini, and A. Golemme, "Measurement of the photorefractive space-charge field in a ferroelectric mesogen", *Appl. Phys. Lett.* **84**, 1034–1036 (2004).
17. J.S. Schildkraut and A.V. Buettner, "Theory and simulation of the formation and erasure of space-charge gratings in photoconductive polymers", *J. Appl. Phys.* **72**, 1888–1893 (1992).
18. J.S. Schildkraut and Y. Cui, "Zero-order and first-order theory of the formation of space-charge gratings in photoconductive polymers", *J. Appl. Phys.* **72**, 5055–5060 (1992).

Photonics Europe 2006

CALL FOR PAPERS

Present and publish your research at the premier European event that supports the convergence of research and commerce



3-7 April 2006

Palais de la Musique et des Congrès
Strasbourg, France

Conferences · Courses · Exhibition



Abstract Due Date
19 September 2005

Lasers

Semiconductor
Solid State

Biophotonics

Nanophotonics

Photonic Crystals

Organic Optoelectronics

Micro- and Nanometrology

Optical Sensing

Micro-Optics and Packaging

MEMS and MOEMS

Photonics in Multimedia

Microwave and Terahertz Photonics

Reliability of Photonic Components

Photon Management

Photonic Integrated Circuits

Photonics for Solar Energy

Photonics for the Automobile

Plus:

Hot Topics

Benefits-to-Industry Programme

EU Framework News & Updates

Manuscript Due
6 March 2006